Design of Linear Clustered Arrays with Non-Contiguous Sub-Arrays through a Total-Variation CS Method

N. Anselmi, G. Gottardi, G. Oliveri, and A. Massa

Abstract

In this work, the design of linear clustered arrays is addressed by means of a novel compressive sensing (*CS*) methodology. More in detail, the synthesis of the beamforming network (*BFN*) is recast within a total-variation (*TV*) formulation aimed at minimizing the discrete gradient of the array excitation weights. A set of representative results is reported to verify the effectiveness of the proposed *TV-CS* methodology when dealing with the design of linear arrays with non-contiguous clusters.

Contents

1 Numerical Results **2**

1.1 Taylor - $SLL = -20dB$ - $N = 40$ 2

1.2 Taylor - $SLL = -20dB$ - $N = 100$ 7

1.3 Taylor - $SLL = -20dB$ - $N = 200$ 12

1 Numerical Results

1.1 Taylor - $SLL = -20dB$ - $N = 40$

Array Geometry:

- Linear Array
- Number of Elements: $N = 40$
- Element Spacing: $\Delta L_{REF} = \lambda/2$
- Aperture Length: $L = 19.5\lambda$

Reference Pattern:

- Pencil Beam, Taylor
- Number of elements: $N = 40$
- Transition Index: $\overline{n} = 6$
- Sidelobe Ratio: $SLL = -20dB$

Pareto Parameters:

- Pattern Samples: $K \in \{4, 6, 8..., 20, 25, ..., 50, 60, 70, ..., 100, 300, 400, 500, 1000\}$
- Primary penalty parameter: $\mu \in \left\{2 \times 10^{-2}, 2 \times 10^{-1}, ..., 2 \times 10^{13}\right\}$
- Secondary penalty parameter: $\beta \in \left\{2 \times 10^{-2}, 2 \times 10^{-1}, ..., 2 \times 10^{13}\right\}$
- $m_t \in \left\{1 \times 10^1, 2 \times 10^1, 5 \times 10^1, 1 \times 10^2, 5 \times 10^2, 1 \times 10^3, 2 \times 10^3\right\}$
- $m_o \in \left\{5 \times 10^0, 5 \times 10^1, 1 \times 10^2, 5 \times 10^2, 1 \times 10^3\right\}$

Clustering Parameters:

- Cluster Magnitude Tolerance: $\tau_C = 1.0 \times 10^{-3}$

TV-CS Parameters:

- Starting primary penalty parameter: $\mu_0 = \mu$ (default)
- Starting secondary penalty parameter: $\beta_0 = \beta$ (default)
- Outer stopping tolerance: $t_o = 1 \times 10^{-3}$ (default)
- Inner stopping tolerance: $t_i = 1 \times 10^{-3}$ (default)

- Isotropic/anisotropic TV flag: $\mathcal{F}_{TV} = 1$
- Negative/Positive signal: $\mathcal{F}_N = [false]$ (default)
- TV/L2 flag:$\mathcal{F}_{T2} = [false]$ (default)
- Real/Imaginary signal flag: $\mathcal{F}_R = [false]$ (default)
- Scaling Matrix A flag: $\mathcal{F}_A = [true]$ (default)
- Scaling Vector B flag: $\mathcal{F}_B = [true]$ (default)
- Guess Solution: $\mathcal{F}_G = 0$ (all zeroes)

RESULTS

Pareto Front:

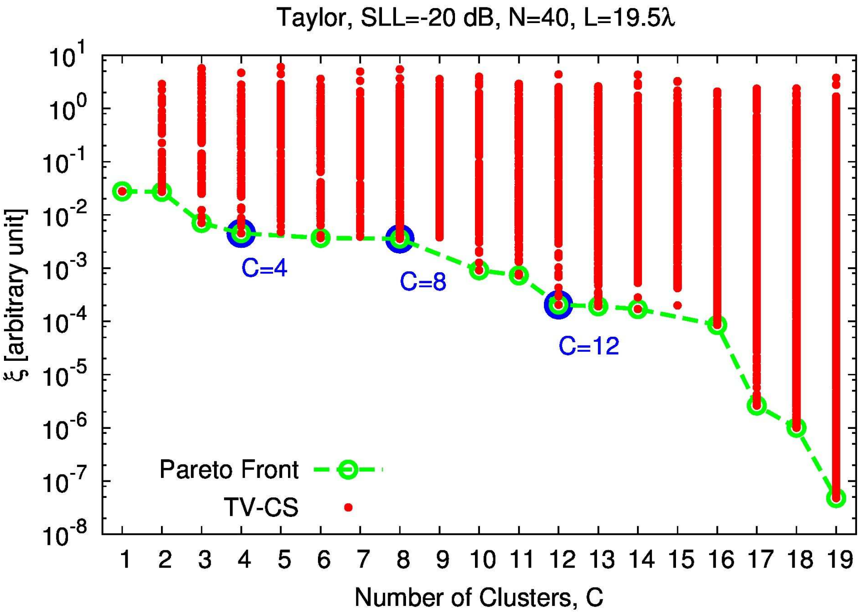

Figure 1: *Performance Assessment* (*Taylor Pattern*, $N = 40$, $SLL = -20$ dB, $d = 0.5\lambda$, $L = 19.5\lambda$)−Pareto front

C	ξ	μ	β	K	m_t	m_o
4	4.52×10^{-3}	2×10^{-2}	2×10^{0}	500	2×10^{3}	1×10^{3}
8	3.56×10^{-3}	2×10^{-2}	2×10^{1}	90	2×10^{3}	5×10^{2}
12	2.05×10^{-4}	2×10^{-2}	2×10^{1}	90	1×10^{3}	5×10^{2}

Table I: *Performance Assessment* (*Taylor Pattern*, $N = 40$, $SLL = -20$ dB, $d = 0.5\lambda$, $L = 19.5\lambda$)−Selected solutions.

Number of Clusters: $C = 4$

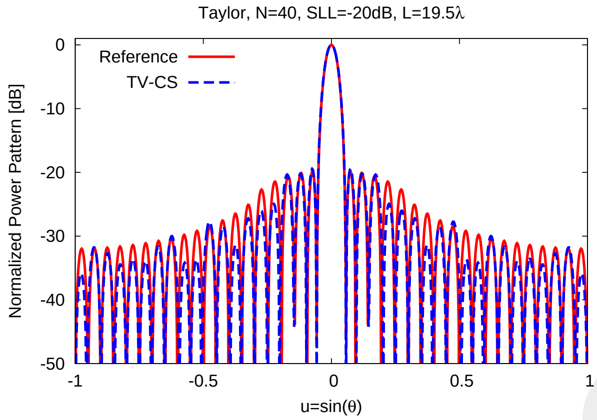

Figure 2: *Performance Assessment* (*Taylor Pattern*, $N = 40$, $SLL = -20$ dB, $d = 0.5\lambda$, $L = 19.5\lambda$, $C = 4$)-—Power pattern.

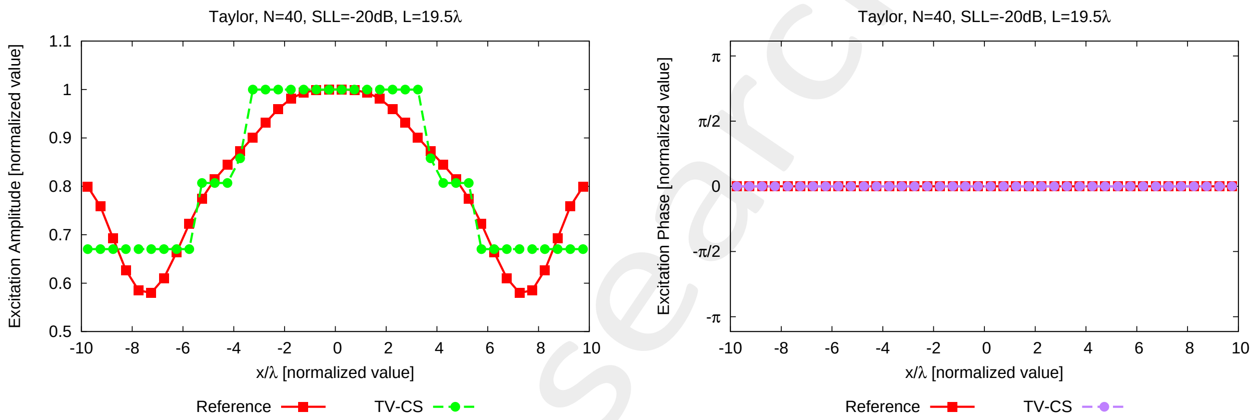

(a) (b)

Figure 3: *Performance Assessment* (*Taylor Pattern*, $N = 40$, $SLL = -20$ dB, $d = 0.5\lambda$, $L = 19.5\lambda$, $C = 4$)-—Excitations amplitude (a) and phase (b).

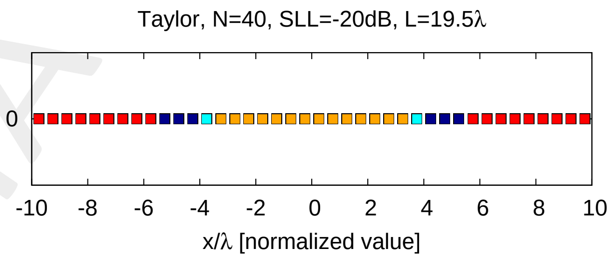

Figure 4: *Performance Assessment* (*Taylor Pattern*, $N = 40$, $SLL = -20$ dB, $d = 0.5\lambda$, $L = 19.5\lambda$, $C = 4$)-—Array elements clustering configuration.

	C	SLL [dB]	BW [deg]	$D_{\max}$ [dB]	DRR_{max}[dB]	ξ [$\times 10^{-3}$]
$Reference$	–	-19.80	2.7114	15.89	2.37	–
$TV-CS$	4	-19.44	2.7447	15.88	1.74	4.52

Table II: *Performance Assessment* (*Taylor Pattern*, $N = 40$, $SLL = -20$ dB, $d = 0.5\lambda$, $L = 19.5\lambda$, $C = 4$)-—Array Performance Indexes.

Number of Clusters: $C = 8$

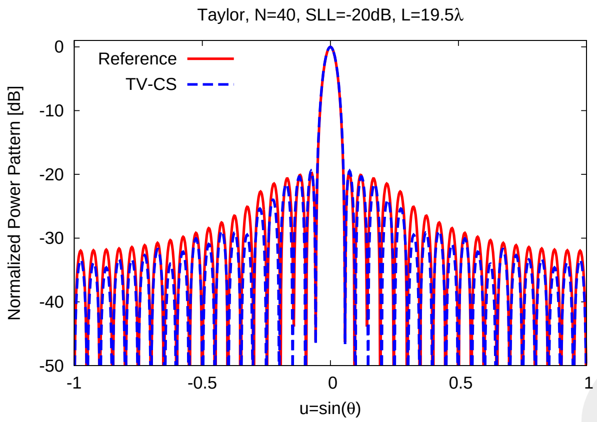

Figure 5: *Performance Assessment* (*Taylor Pattern*, $N = 40$, $SLL = -20$ dB, $d = 0.5\lambda$, $L = 19.5\lambda$, $C = 8$)-−Power pattern

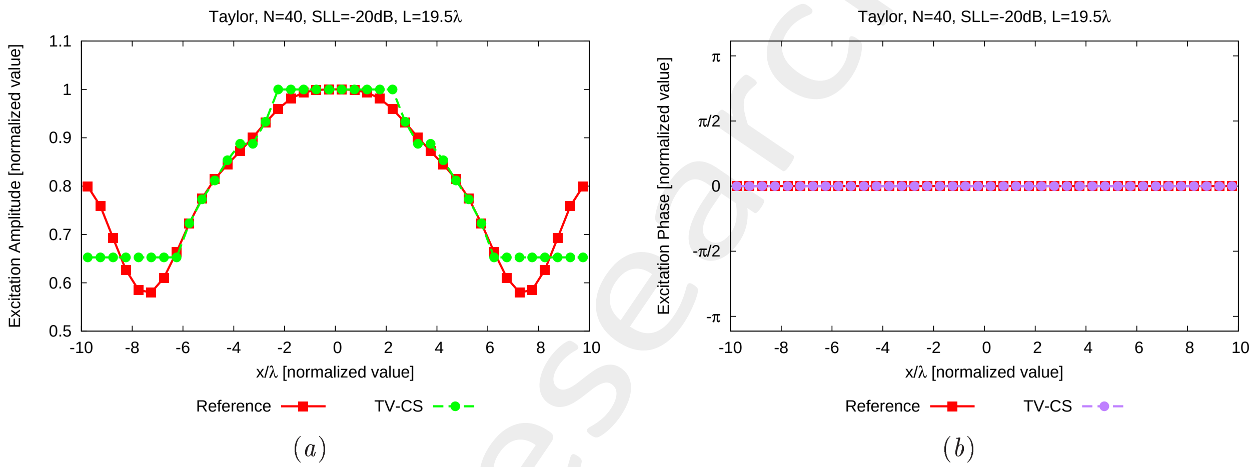

Figure 6: *Performance Assessment* (*Taylor Pattern*, $N = 40$, $SLL = -20$ dB, $d = 0.5\lambda$, $L = 19.5\lambda$, $C = 8$)-−Excitations amplitude (a) and phase (b).

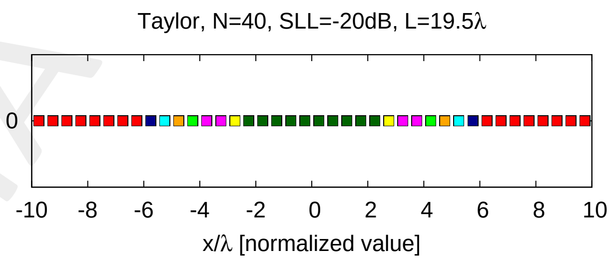

Figure 7: *Performance Assessment* (*Taylor Pattern*, $N = 40$, $SLL = -20$ dB, $d = 0.5\lambda$, $L = 19.5\lambda$, $C = 8$)-−Array elements clustering configuration.

	C	SLL [dB]	BW [deg]	$D_{\max}$ [dB]	DRR_{max}[dB]	ξ [$\times 10^{-3}$]
$Reference$	$-$	-19.80	2.7114	15.89	2.37	$-$
$TV-CS$	8	-19.46	2.7523	15.88	1.85	3.56

Table III: *Performance Assessment* (*Taylor Pattern*, $N = 40$, $SLL = -20$ dB, $d = 0.5\lambda$, $L = 19.5\lambda$, $C = 8$)-−Array Performance Indexes.

Number of Clusters: $C = 12$

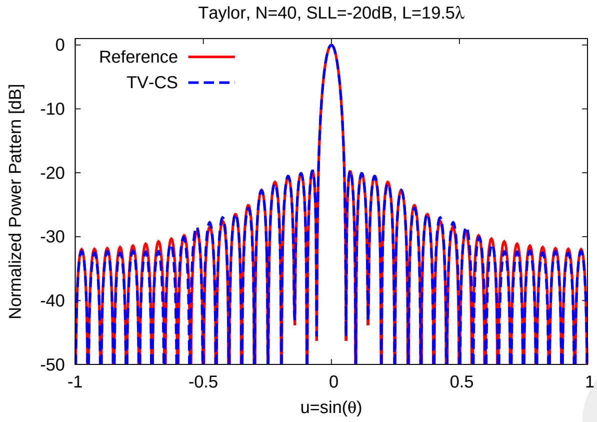

Figure 8: *Performance Assessment* (*Taylor Pattern*, $N = 40$, $SLL = -20$ dB, $d = 0.5\lambda$, $L = 19.5\lambda$, $C = 12$)-—Power pattern.

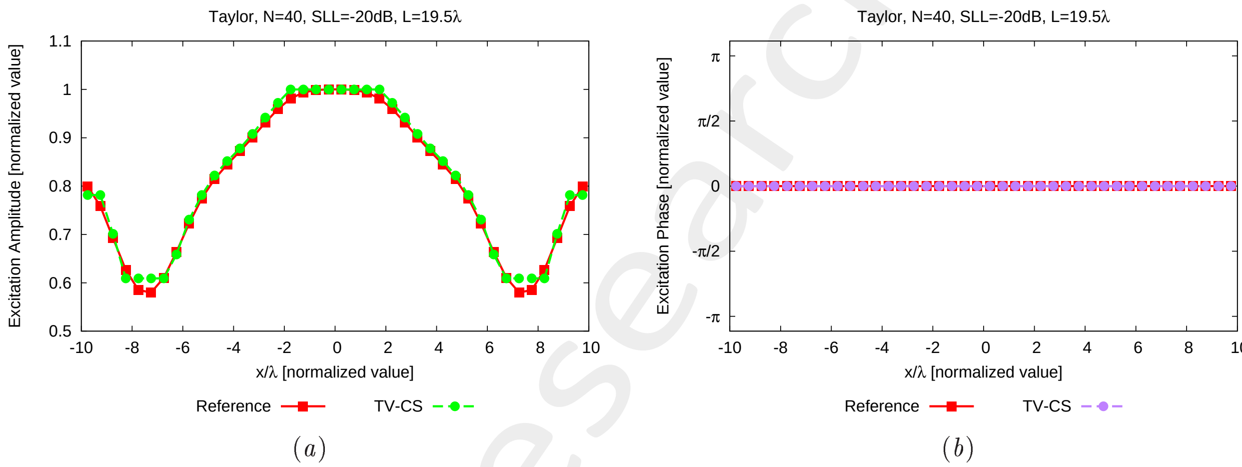

Figure 9: *Performance Assessment* (*Taylor Pattern*, $N = 40$, $SLL = -20$ dB, $d = 0.5\lambda$, $L = 19.5\lambda$, $C = 12$)-—Excitations amplitude (a) and phase (b).

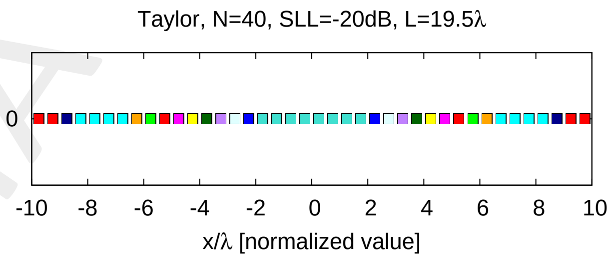

Figure 10: *Performance Assessment* (*Taylor Pattern*, $N = 40$, $SLL = -20$ dB, $d = 0.5\lambda$, $L = 19.5\lambda$, $C = 12$)-—Array elements clustering configuration.

	C	SLL [dB]	BW [deg]	$D_{\max}$ [dB]	DRR_{max}[dB]	ξ [$\times 10^{-4}$]
$Reference$	–	-19.80	2.7114	15.89	2.37	–
$TV-CS$	12	-19.71	2.7123	15.89	2.15	2.05

Table IV: *Performance Assessment* (*Taylor Pattern*, $N = 40$, $SLL = -20$ dB, $d = 0.5\lambda$, $L = 19.5\lambda$, $C = 12$)-—Array Performance Indexes.

1.2 Taylor - $SLL = -20dB$ - $N = 100$

Array Geometry:

- Linear Array
- Number of Elements: $N = 100$
- Element Spacing: $\Delta L_{REF} = \lambda/2$
- Aperture Length: $L = 49.5\lambda$

Reference Pattern:

- Pencil Beam, Taylor
- Number of elements: $N = 100$
- Transition Index: $\overline{n} = 6$
- Sidelobe Ratio: $SLL = -20dB$

Pareto Parameters:

- Pattern Samples: $K \in \{4, 6, 8..., 20, 25, ..., 50, 60, 70, ..., 100, 300, 400, 500, 1000\}$
- Primary penalty parameter: $\mu \in \left\{2 \times 10^{-2}, 2 \times 10^{-1}, ..., 2 \times 10^{13}\right\}$
- Secondary penalty parameter: $\beta \in \left\{2 \times 10^{-2}, 2 \times 10^{-1}, ..., 2 \times 10^{13}\right\}$
- $m_t \in \left\{1 \times 10^1, 2 \times 10^1, 5 \times 10^1, 1 \times 10^2, 5 \times 10^2, 1 \times 10^3, 2 \times 10^3\right\}$
- $m_o \in \left\{5 \times 10^0, 5 \times 10^1, 1 \times 10^2, 5 \times 10^2, 1 \times 10^3\right\}$

Clustering Parameters:

- Cluster Magnitude Tolerance: $\tau_C = 1.0 \times 10^{-3}$

TV-CS Parameters:

- Starting primary penalty parameter: $\mu_0 = \mu$ (default)
- Starting secondary penalty parameter: $\beta_0 = \beta$ (default)
- Outer stopping tolerance: $t_o = 1 \times 10^{-3}$ (default)
- Inner stopping tolerance: $t_i = 1 \times 10^{-3}$ (default)
- Isotropic/anisotropic TV flag: $\mathcal{F}_{TV} = 1$
- Negative/Positive signal: $\mathcal{F}_N = [false]$ (default)

- TV/L2 flag:$\mathcal{F}_{T2} = [false]$ (default)
- Real/Imaginary signal flag: $\mathcal{F}_R = [false]$ (default)
- Scaling Matrix A flag: $\mathcal{F}_A = [true]$ (default)
- Scaling Vector B flag: $\mathcal{F}_B = [true]$ (default)
- Guess Solution: $\mathcal{F}_G = 0$ (all zeroes)

RESULTS

Pareto Front:

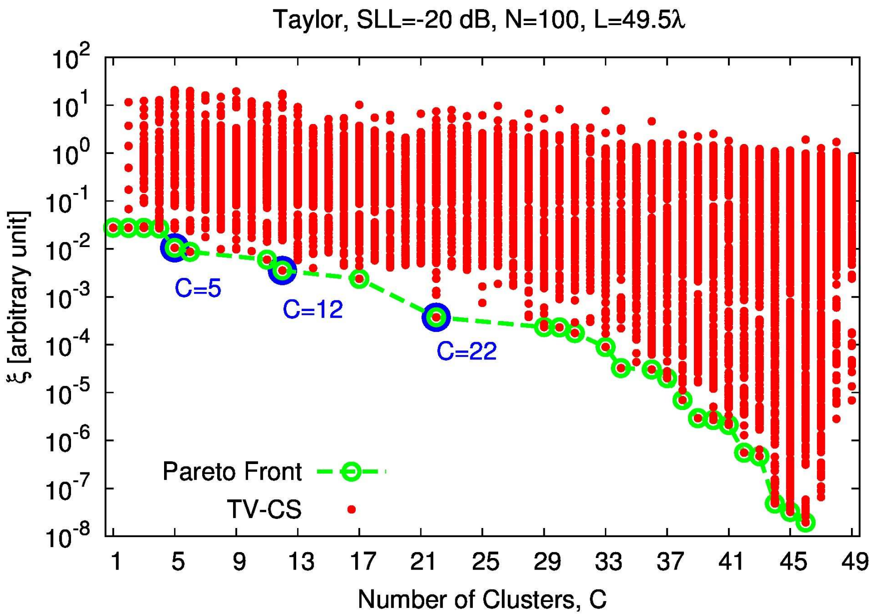

Figure 11: *Performance Assessment* (*Taylor Pattern*, $N = 100$, $SLL = -20$ dB, $d = 0.5\lambda$, $L == 49.5\lambda$)−Pareto front.

C	ξ	μ	β	K	m_t	m_o
5	1.05×10^{-2}	2×10^{-2}	$2 \times 10^{+1}$	60	1000	500
12	3.54×10^{-3}	2×10^{-2}	$2 \times 10^{+1}$	95	2000	1000
22	3.73×10^{-4}	2×10^{-1}	$2 \times 10^{+1}$	200	500	100

Table V: *Performance Assessment* (*Taylor Pattern*, $N = 100$, $SLL = -20$ dB, $d = 0.5\lambda$, $L = 49.5\lambda$)−Selected solutions.

Number of Clusters: $C = 5$

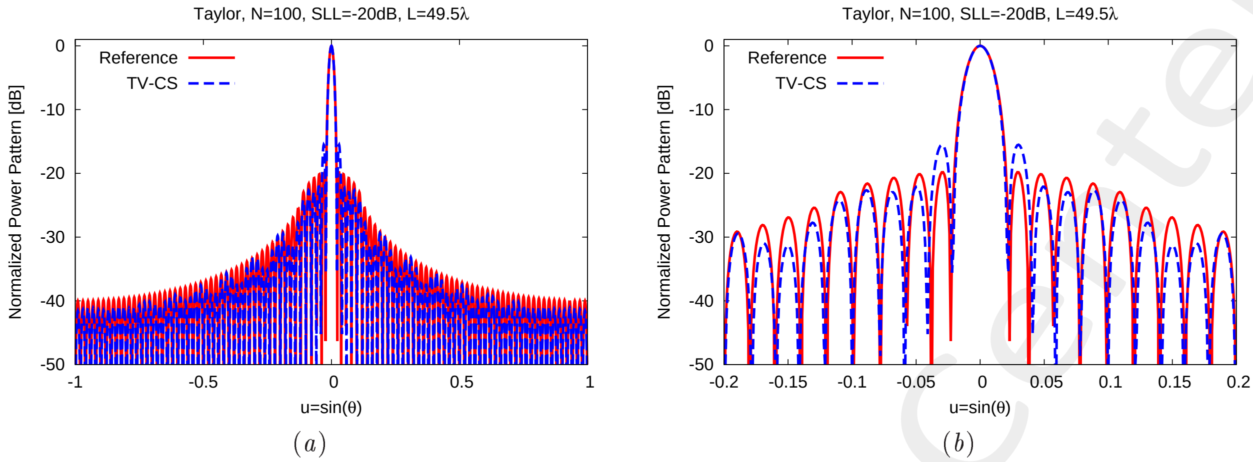

Figure 12: *Performance Assessment* (*Taylor Pattern*, $N = 100$, $SLL = -20$ dB, $d = 0.5\lambda$, $L = 49.5\lambda$, $C = 5$)-−Power pattern over the whole visible $u-$range (a) and a detail of the main lobe (b).

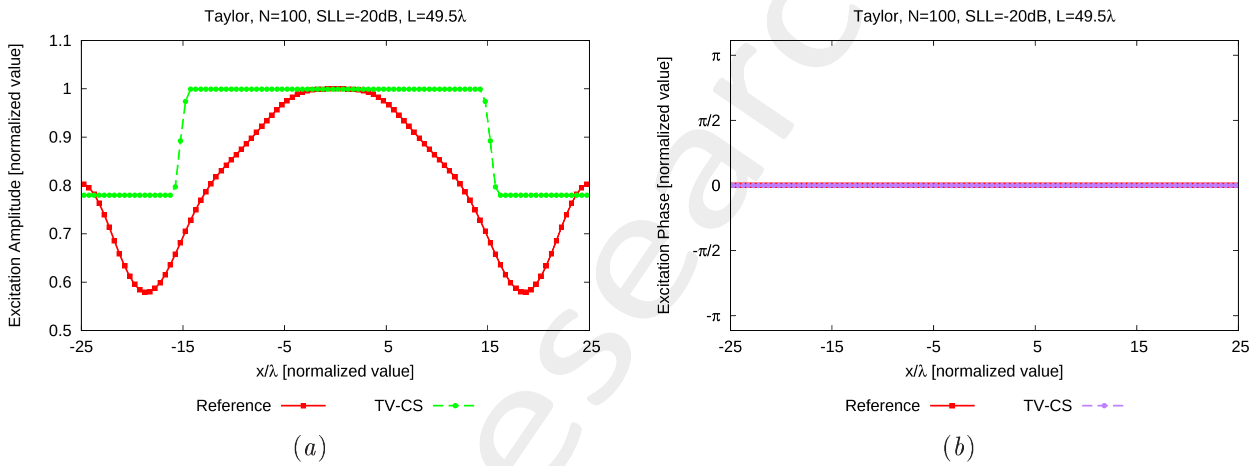

Figure 13: *Performance Assessment* (*Taylor Pattern*, $N = 100$, $SLL = -20$ dB, $d = 0.5\lambda$, $L = 49.5\lambda$, $C = 5$)-−Excitations amplitude (a) and phase (b).

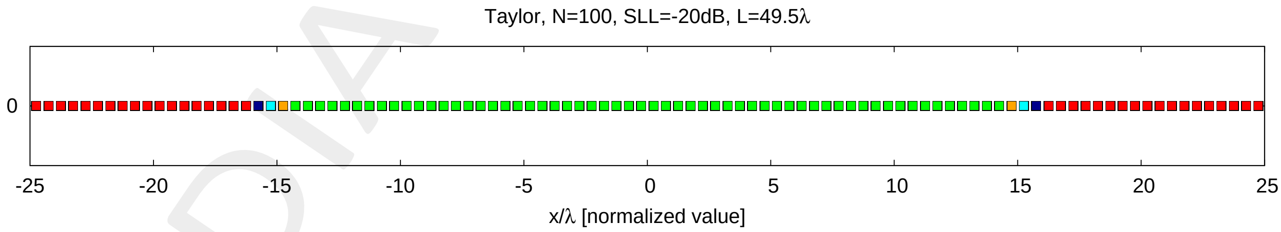

Figure 14: *Performance Assessment* (*Taylor Pattern*, $N = 100$, $SLL = -20$ dB, $d = 0.5\lambda$, $L = 49.5\lambda$, $C = 5$)-−Array elements clustering configuration.

	C	SLL [dB]	BW [deg]	$D_{\max}$ [dB]	DRR_{max}[dB]	ξ [$\times 10^{-2}$]
$Reference$	−	−19.82	1.0842	19.87	2.37	−
$TV-CS$	5	−15.51	1.0654	19.94	1.08	1.05

Table VI: *Performance Assessment* (*Taylor Pattern*, $N = 100$, $SLL = -20$ dB, $d = 0.5\lambda$, $L = 49.5\lambda$, $C = 5$)-−Array Performance Indexes.

Number of Clusters: $C = 12$

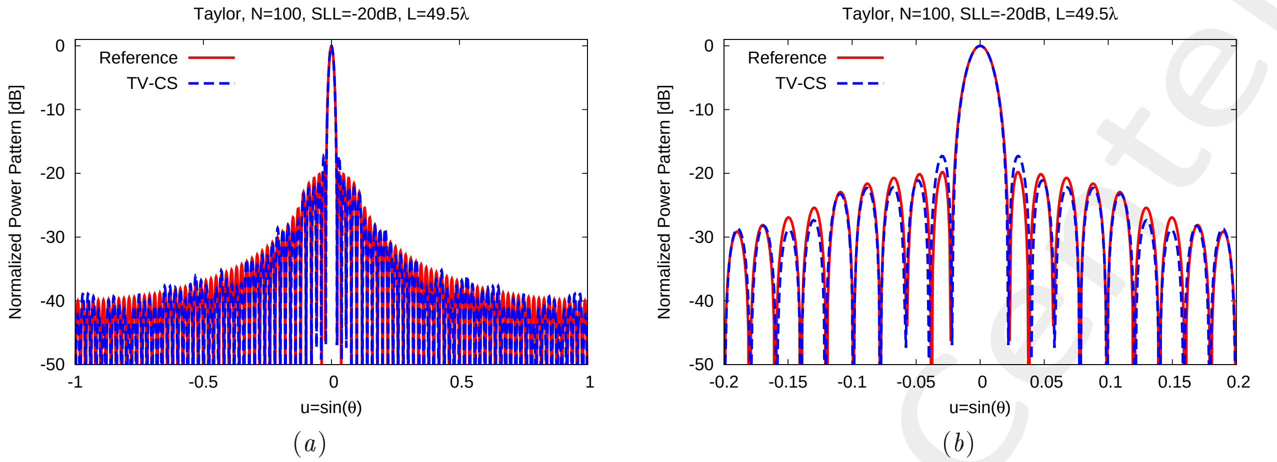

Figure 15: *Performance Assessment* (*Taylor Pattern*, $N = 100$, $SLL = -20$ dB, $d = 0.5\lambda$, $L = 49.5\lambda$, $C = 12$)-−Power pattern over the whole visible $u-$range (a) and a detail of the main lobe (b)

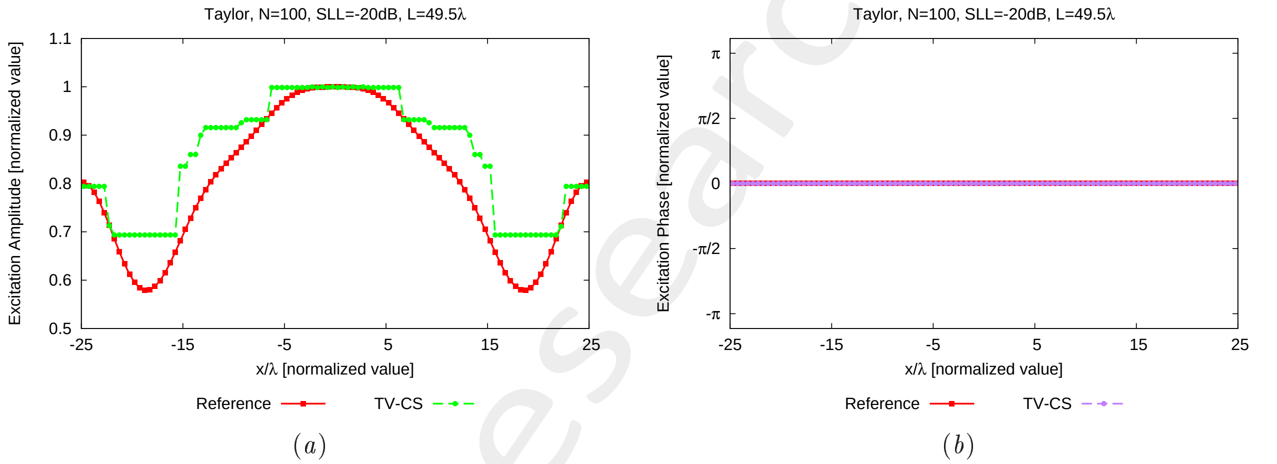

Figure 16: *Performance Assessment* (*Taylor Pattern*, $N = 100$, $SLL = -20$ dB, $d = 0.5\lambda$, $L = 49.5\lambda$, $C = 12$)-−Excitations amplitude (a) and phase (b).

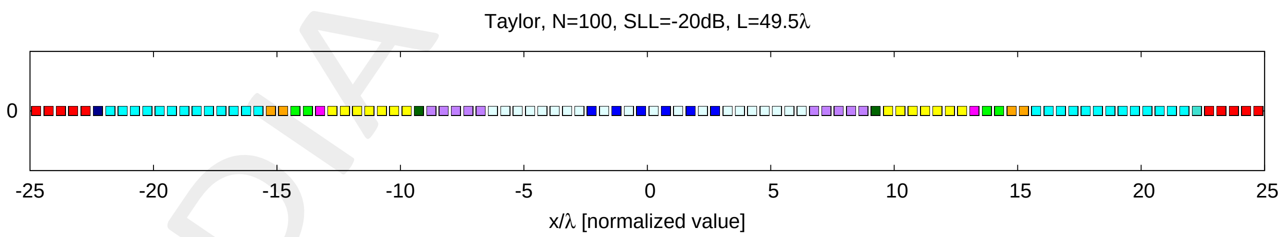

Figure 17: *Performance Assessment* (*Taylor Pattern*, $N = 100$, $SLL = -20$ dB, $d = 0.5\lambda$, $L = 49.5\lambda$, $C = 12$)-−Array elements clustering configuration.

	C	SLL [dB]	BW [deg]	$D_{\max}$ [dB]	DRR_{max}[dB]	ξ [$\times 10^{-3}$]
$Reference$	−	−19.82	1.0842	19.87	2.37	−
$TV-CS$	12	−17.29	1.0736	19.91	1.59	3.54

Table VII: *Performance Assessment* (*Taylor Pattern*, $N = 100$, $SLL = -20$ dB, $d = 0.5\lambda$, $L = 49.5\lambda$, $C = 12$)-−Array Performance Indexes.

Number of Clusters: $C = 22$

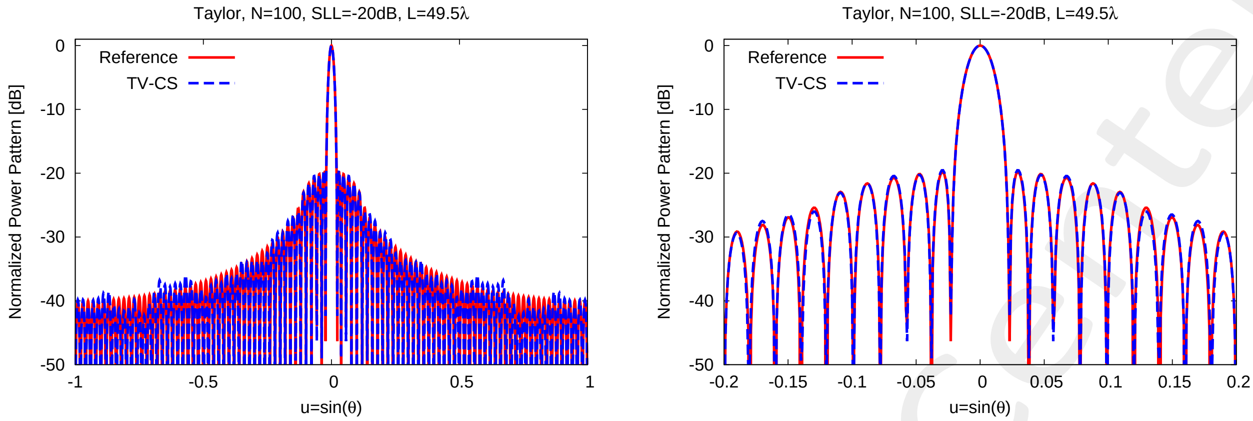

(*a*) (*b*)

Figure 18: *Performance Assessment* (*Taylor Pattern*, $N = 100$, $SLL = -20$ dB, $d = 0.5\lambda$, $L = 49.5\lambda$, $C = 22$)-−Power pattern over the whole visible $u-$range (a) and a detail of the main lobe (b)

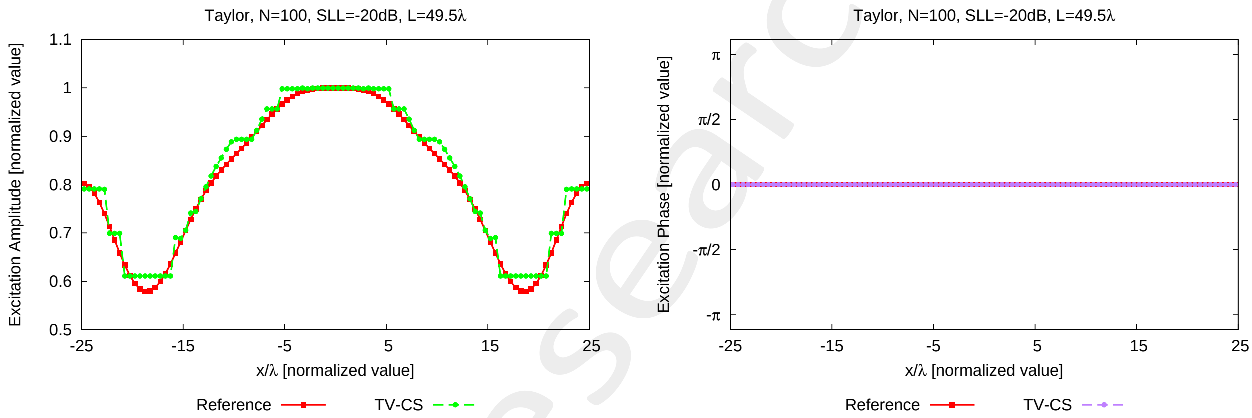

(*a*) (*b*)

Figure 19: *Performance Assessment* (*Taylor Pattern*, $N = 100$, $SLL = -20$ dB, $d = 0.5\lambda$, $L = 49.5\lambda$, $C = 22$)-−Excitations amplitude (a) and phase (b).

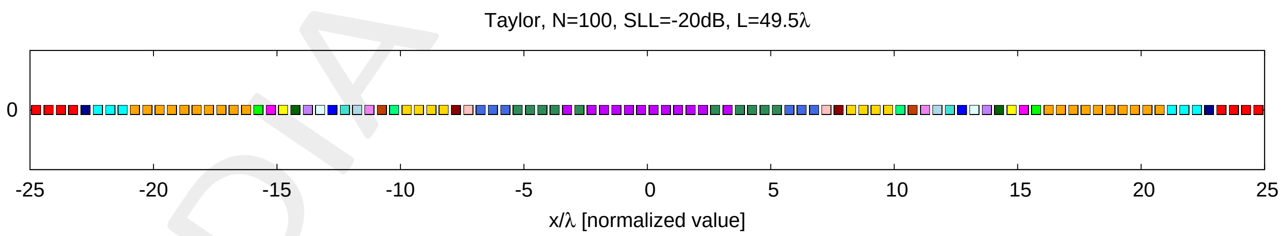

Figure 20: *Performance Assessment* (*Taylor Pattern*, $N = 100$, $SLL = -20$ dB, $d = 0.5\lambda$, $L = 49.5\lambda$, $C = 22$)-−Array elements clustering configuration.

	C	SLL [dB]	BW [deg]	$D_{\max}$ [dB]	DRR_{max}[dB]	ξ [$\times 10^{-4}$]
$Reference$	−	−19.82	1.0842	19.87	2.37	−
$TV-CS$	22	−19.54	1.0736	19.92	2.14	3.73

Table VIII: *Performance Assessment* (*Taylor Pattern*, $N = 100$, $SLL = -20$ dB, $d = 0.5\lambda$, $L = 49.5\lambda$, $C = 22$)−Array Performance Indexes.

1.3 Taylor - $SLL = -20dB$ - $N = 200$

Array Geometry:

- Linear Array
- Number of Elements: $N = 200$
- Element Spacing: $\Delta L_{REF} = \lambda/2$
- Aperture Length: $L = 99.5\lambda$

Reference Pattern:

- Pencil Beam, Taylor
- Number of elements: $N = 200$
- Transition Index: $\overline{n} = 6$
- Sidelobe Ratio: $SLL = -20dB$

Pareto Parameters:

- Pattern Samples: $K \in \{4, 6, 8..., 20, 25, ..., 50, 60, 70, ..., 100, 300, 400, 500, 1000\}$
- Primary penalty parameter: $\mu \in \left\{2 \times 10^{-2}, 2 \times 10^{-1}, ..., 2 \times 10^{13}\right\}$
- Secondary penalty parameter: $\beta \in \left\{2 \times 10^{-2}, 2 \times 10^{-1}, ..., 2 \times 10^{13}\right\}$
- $m_t \in \left\{1 \times 10^1, 2 \times 10^1, 5 \times 10^1, 1 \times 10^2, 5 \times 10^2, 1 \times 10^3, 2 \times 10^3\right\}$
- $m_o \in \left\{5 \times 10^0, 5 \times 10^1, 1 \times 10^2, 5 \times 10^2, 1 \times 10^3\right\}$

Clustering Parameters:

- Cluster Magnitude Tolerance: $\tau_C = 1.0 \times 10^{-3}$

TV-CS Parameters:

- Starting primary penalty parameter: $\mu_0 = \mu$ (default)
- Starting secondary penalty parameter: $\beta_0 = \beta$ (default)
- Outer stopping tolerance: $t_o = 1 \times 10^{-3}$ (default)
- Inner stopping tolerance: $t_i = 1 \times 10^{-3}$ (default)
- Isotropic/anisotropic TV flag: $\mathcal{F}_{TV} = 1$
- Negative/Positive signal: $\mathcal{F}_N = [false]$ (default)

- TV/L2 flag:$\mathcal{F}_{T2} = [false]$ (default)

- Real/Imaginary signal flag: $\mathcal{F}_R = [false]$ (default)

- Scaling Matrix A flag: $\mathcal{F}_A = [true]$ (default)

- Scaling Vector B flag: $\mathcal{F}_B = [true]$ (default)

- Guess Solution: $\mathcal{F}_G = 0$ (all zeroes)

RESULTS

Pareto Front:

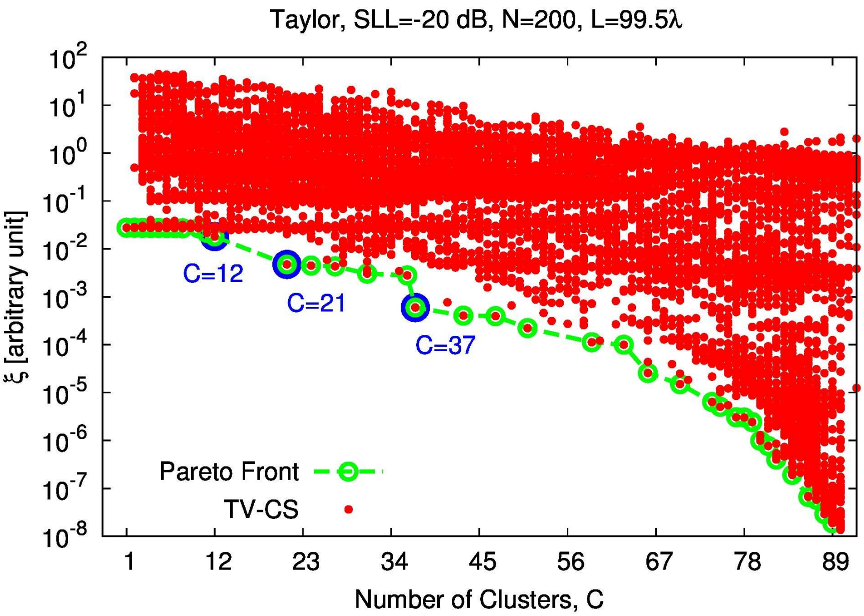

Figure 21: *Performance Assessment* (*Taylor Pattern*, $N = 200$, $SLL = -20$ dB, $d = 0.5\lambda$, $L = 99.5\lambda$)−Pareto front.

C	ξ	μ	β	K	m_t	m_o
12	1.81×10^{-2}	2×10^{-2}	$2 \times 10^{+1}$	40	2×10^{3}	1×10^{3}
21	4.73×10^{-3}	2×10^{-2}	$2 \times 10^{+1}$	80	2×10^{3}	1×10^{3}
37	5.97×10^{-4}	2×10^{-2}	$2 \times 10^{+1}$	1000	1×10^{3}	5×10^{2}

Table IX: *Performance Assessment* (*Taylor Pattern*, $N = 200$, $SLL = -20$ dB, $d = 0.5\lambda$, $L = 99.5\lambda$)−Selected solutions.

Number of Clusters: $C = 12$

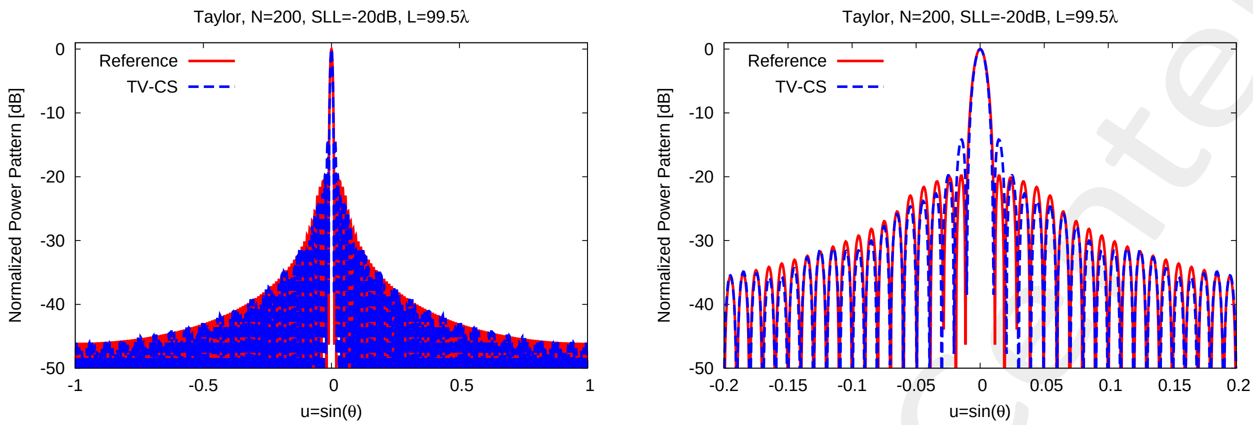

(a) (b)

Figure 22: *Performance Assessment* (*Taylor Pattern*, $N = 200$, $SLL = -20$ dB, $d = 0.5\lambda$, $L = 99.5\lambda$, $C = 12$)-—Power pattern over the whole visible $u-$range (a) and a detail of the main lobe (b)

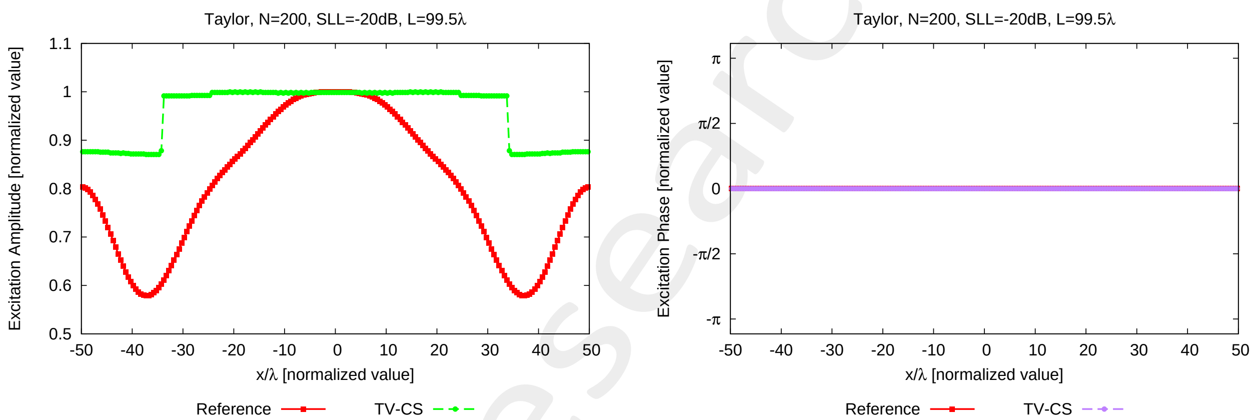

(a) (b)

Figure 23: *Performance Assessment* (*Taylor Pattern*, $N = 200$, $SLL = -20$ dB, $d = 0.5\lambda$, $L = 99.5\lambda$, $C = 12$)-—Excitations amplitude (a) and phase (b).

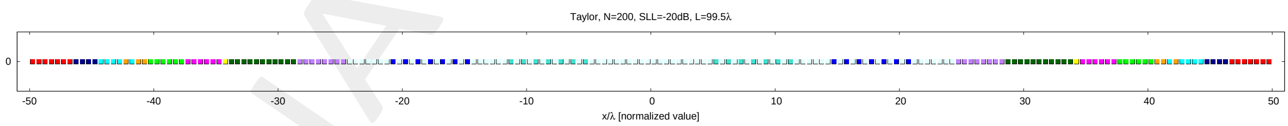

Figure 24: *Performance Assessment* (*Taylor Pattern*, $N = 200$, $SLL = -20$ dB, $d = 0.5\lambda$, $L = 99.5\lambda$, $C = 12$)-—Array elements clustering configuration.

	C	SLL [dB]	BW [deg]	$D_{\max}$ [dB]	DRR_{max}[dB]	ξ [$\times 10^{-2}$]
$Reference$	–	-19.82	0.5421	22.87	2.37	–
$TV-CS$	12	-14.18	0.5197	22.99	0.60	1.81

Table X: *Performance Assessment* (*Taylor Pattern*, $N = 200$, $SLL = -20$ dB, $d = 0.5\lambda$, $L = 99.5\lambda$, $C = 12$)-—Array Performance Indexes.

Number of Clusters: $C = 21$

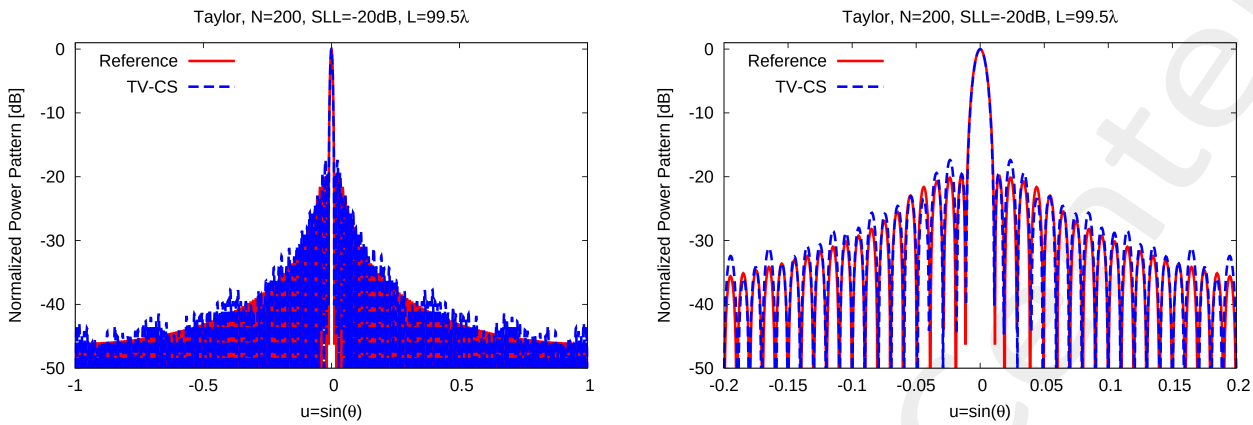

(a) (b)

Figure 25: *Performance Assessment* (*Taylor Pattern*, $N = 200$, $SLL = -20$ dB, $d = 0.5\lambda$, $L = 99.5\lambda$, $C = 21$)-
$-$Power pattern over the whole visible $u-$range (a) and a detail of the main lobe (b)

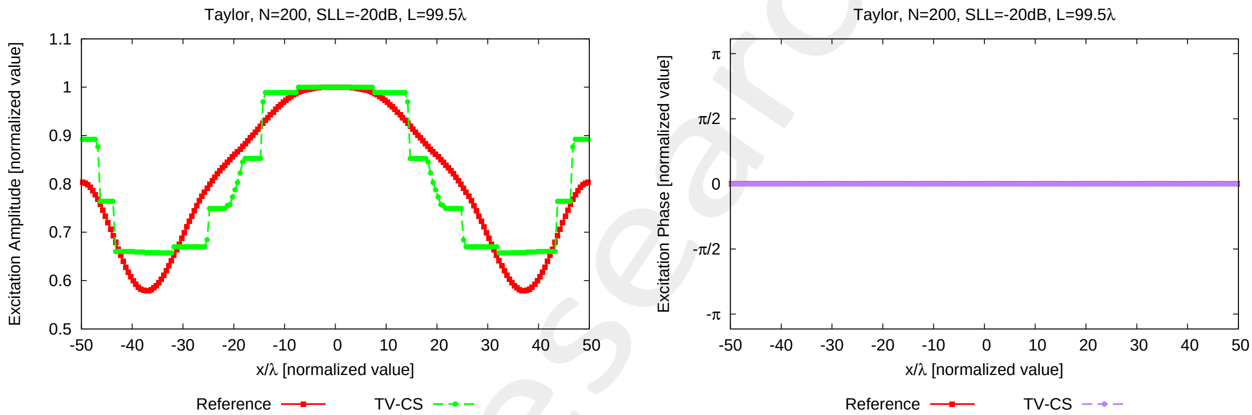

(a) (b)

Figure 26: *Performance Assessment* (*Taylor Pattern*, $N = 200$, $SLL = -20$ dB, $d = 0.5\lambda$, $L = 99.5\lambda$, $C = 21$)-
$-$Excitations amplitude (a) and phase (b).

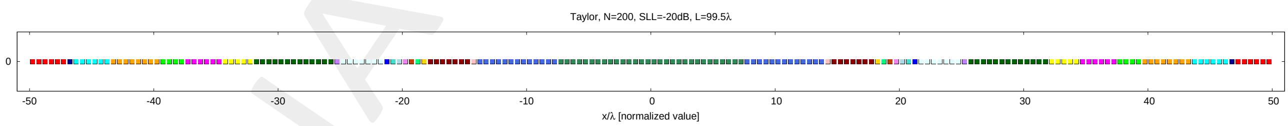

Figure 27: *Performance Assessment* (*Taylor Pattern*, $N = 200$, $SLL = -20$ dB, $d = 0.5\lambda$, $L = 99.5\lambda$, $C = 21$)-
$-$Array elements clustering configuration.

	C	SLL [dB]	BW [deg]	$D_{\max}$ [dB]	DRR_{max}[dB]	ξ [$\times 10^{-3}$]
$Reference$	$-$	-19.82	0.5421	22.87	2.37	$-$
$TV-CS$	21	-17.37	0.5317	22.89	1.82	4.73

Table XI: *Performance Assessment* (*Taylor Pattern*, $N = 200$, $SLL = -20$ dB, $d = 0.5\lambda$, $L = 99.5\lambda$, $C = 21$)-
$-$Array Performance Indexes.

Number of Clusters: $C = 37$

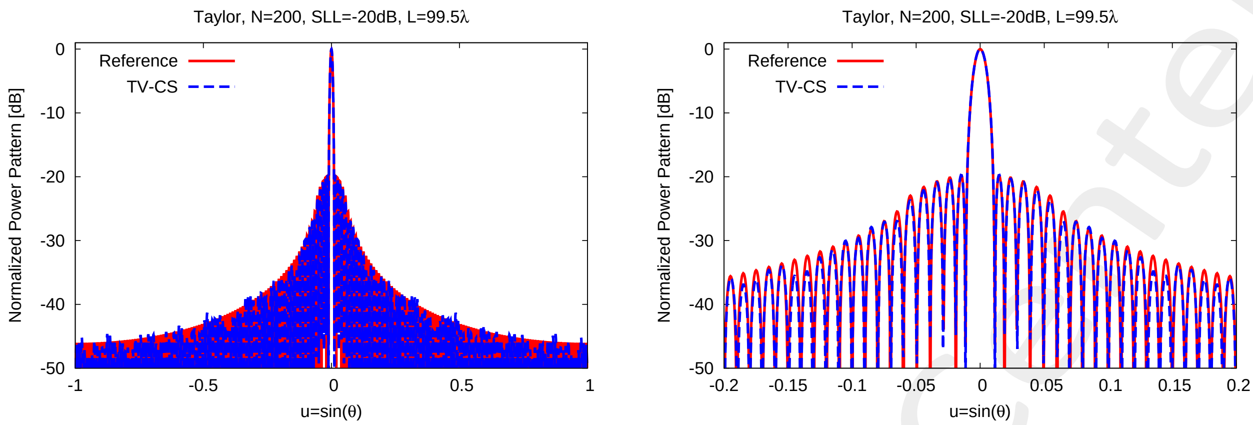

(a) (b)

Figure 28: *Performance Assessment* (*Taylor Pattern*, $N = 200$, $SLL = -20$ dB, $d = 0.5\lambda$, $L = 99.5\lambda$, $C = 37$)-–Power pattern over the whole visible u–range (a) and a detail of the main lobe (b)

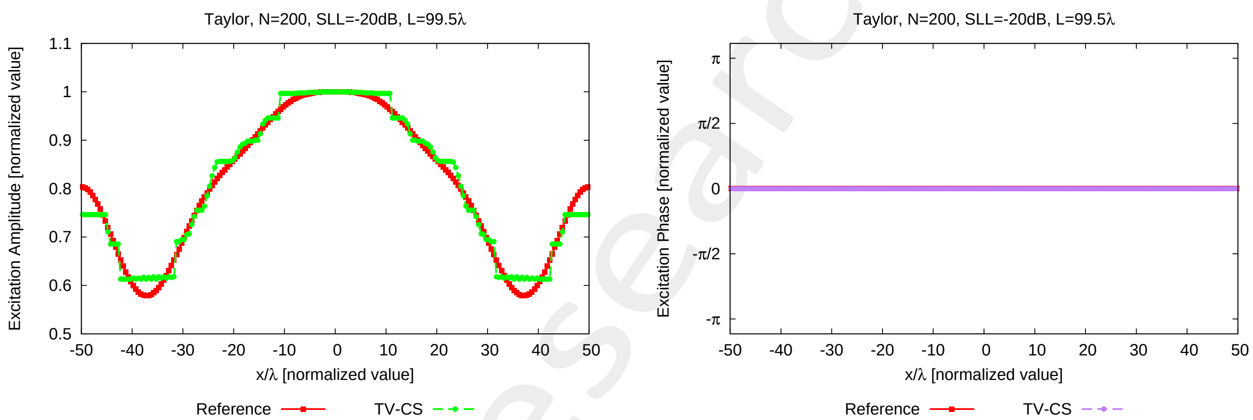

(a) (b)

Figure 29: *Performance Assessment* (*Taylor Pattern*, $N = 200$, $SLL = -20$ dB, $d = 0.5\lambda$, $L = 99.5\lambda$, $C = 37$)-–Excitations amplitude (a) and phase (b).

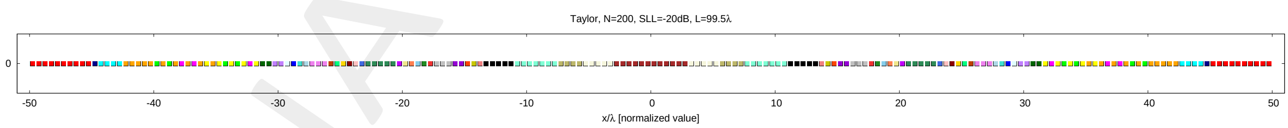

Figure 30: *Performance Assessment* (*Taylor Pattern*, $N = 200$, $SLL = -20$ dB, $d = 0.5\lambda$, $L = 99.5\lambda$, $C = 37$)-–Array elements clustering configuration.

	C	SLL [dB]	BW [deg]	$D_{\max}$ [dB]	DRR_{max}[dB]	ξ [$\times 10^{-4}$]
Reference	–	-19.82	0.5421	22.87	2.37	–
TV – CS	37	-19.74	0.5446	22.88	2.12	5.97

Table XII: *Performance Assessment* (*Taylor Pattern*, $N = 200$, $SLL = -20$ dB, $d = 0.5\lambda$, $L = 99.5\lambda$, $C = 37$)-–Array Performance Indexes.

References

[1] P. Rocca, G. Oliveri, R. J. Mailloux, and A. Massa, "Unconventional phased array architectures and design methodologies - A Review," *Proc. IEEE*, vol. 104, no. 3, pp. 544-560, Mar. 2016.

[2] G. Oliveri, G. Gottardi, F. Robol, A. Polo, L. Poli, M. Salucci, M. Chuan, C. Massagrande, P. Vinetti, M. Mattivi, R. Lombardi, and A. Massa, "Co-design of unconventional array architectures and antenna elements for *5G* base stations," *IEEE Trans. Antennas Propag.*, vol. 65, no. 12, pp. 6752-6767, Dec. 2017.

[3] N. Anselmi, P. Rocca, M. Salucci, and A. Massa, "Irregular phased array tiling by means of analytic schemata-driven optimization," *IEEE Trans. Antennas Propag.*, vol. 65, no. 9, pp. 4495-4510, Sep. 2017.

[4] G. Oliveri, "Multi-beam antenna arrays with common sub-array layouts," *IEEE Antennas Wireless Propag. Lett.*, vol. 9, pp. 1190-1193, 2010.

[5] P. Rocca, R. Haupt, and A. Massa, "Sidelobe reduction through element phase control in sub-arrayed array antennas," *IEEE Antennas Wireless Propag. Lett.*, vol. 8, pp. 437-440, 2009.

[6] P. Rocca, L. Manica, R. Azaro, and A. Massa, "A hybrid approach for the synthesis of sub-arrayed monopulse linear arrays," *IEEE Trans. Antennas Propag.*, vol. 57, no. 1, pp. 280-283, Jan. 2009.

[7] G. Oliveri, P. Rocca, and A. Massa, "Reliable diagnosis of large linear arrays - a Bayesian compressive sensing approach," *IEEE Trans. Antennas Propag.*, vol. 60, no. 10, pp. 4627-4636, Oct. 2012.

[8] A. Massa, P. Rocca, and G. Oliveri, "Compressive sensing in electromagnetics - A review," *IEEE Antennas Propag. Mag.*, pp. 224-238, vol. 57, no. 1, Feb. 2015.

[9] G. Oliveri, M. Salucci, N. Anselmi, and A. Massa, "Compressive sensing as applied to inverse problems for imaging: theory, applications, current trends, and open challenges," *IEEE Antennas Propag. Mag.*, vol. 59, no. 5, pp. 34-46, Oct. 2017.

[10] P. Rocca, M. A. Hannan, M. Salucci, and A. Massa, "Single-snapshot DoA estimation in array antennas with mutual coupling through a multi-scaling Bayesian compressive sensing strategy," *IEEE Trans. Antennas Propag.*, vol. 65, no. 6, pp. 3203-3213, Jun. 2017.

[11] L. Poli, G. Oliveri, P. Rocca, M. Salucci, and A. Massa, "Long-distance WPT unconventional arrays synthesis," *J. Electromagn. Waves Appl.*, vol. 31, no. 14, pp. 1399-1420, Jul. 2017.

[12] G. Oliveri, M. Salucci, and A. Massa, "Synthesis of modular contiguously clustered linear arrays through a sparseness-regularized solver," *IEEE Trans. Antennas Propag.*, vol. 64, no. 10, pp. 4277-4287, Oct. 2016.

[13] F. Viani, G. Oliveri, and A. Massa, "Compressive sensing pattern matching techniques for synthesizing planar sparse arrays," *IEEE Trans. Antennas Propag.*, vol. 61, no. 9, pp. 4577-4587, Sept. 2013.

[14] G. Oliveri and A. Massa, "Bayesian compressive sampling for pattern synthesis with maximally sparse non-uniform linear arrays," *IEEE Trans. Antennas Propag.*, vol. 59, no. 2, pp. 467-481, Feb. 2011.

[15] N. Anselmi, G. Oliveri, M. A. Hannan, M. Salucci, and A. Massa, “Color compressive sensing imaging of arbitrary-shaped scatterers,” *IEEE Trans. Microw. Theory Techn.*, vol. 65, no. 6, pp. 1986-1999, Jun. 2017.

[16] N. Anselmi, G. Oliveri, M. Salucci, and A. Massa, “Wavelet-based compressive imaging of sparse targets,” *IEEE Trans. Antennas Propag.*, vol. 63, no. 11, pp. 4889-4900, Nov. 2015.

[17] G. Oliveri, N. Anselmi, and A. Massa, "Compressive sensing imaging of non-sparse 2D scatterers by a total-variation approach within the Born approximation," *IEEE Trans. Antennas Propag.*, vol. 62, no. 10, pp. 5157-5170, Oct. 2014.

[18] N. Anselmi, G. Gottardi, G. Oliveri, and A. Massa, "A total-variation sparseness-promoting method for the synthesis of contiguously clustered linear architectures" *IEEE Trans. Antennas Propag.*, vol. 67, no. 7, pp. 4589-4601, Jul. 2019.

[19] M. Salucci, A. Gelmini, G. Oliveri, and A. Massa, "Planar arrays diagnosis by means of an advanced Bayesian compressive processing," *IEEE Tran. Antennas Propag.*, vol. 66, no. 11, pp. 5892-5906, Nov. 2018.